Fusion Engineering and Design 86 (2011) 623–626

Contents lists available at ScienceDirect

Fusion Engineering and Design

journal homepage: www.elsevier.com/locate/fusengdes

Structural analysis of the JT-60SA cryostat base

Esther Rincón[a,*], Javier Alonso[a], Germán Barrera[a], José Botija[a], Pilar Fernández[a], Mercedes Medrano[a], Germán Pérez[a], Francisco Ramos[a], Alfonso Soleto[a], Pietro Barabaschi[b], Enrico Di Pietro[b], Lionel Meunier[b], Akira Sakasai[c], Kei Masaki[c], Yusuke Shibama[c]

[a] Association EURATOM - CIEMAT, Avda. Complutense 22, 28040 Madrid, Spain
[b] Fusion for Energy, JT-60SA European Home Team, 85748 Garching bei Munchen, Germany
[c] JAEA, Japan Atomic Energy Agency, Naka Fusion Institute, Ibaraki 311-0193, Japan

ARTICLE INFO

Article history:
Available online 12 February 2011

Keywords:
JT-60SA
Cryostat
Cryostat base
Structural analysis
Limit analysis
ANSYS

ABSTRACT

Design and manufacturing of the JT-60SA cryostat is being performed by CIEMAT, according to the Broader Approach Agreement between Japan and the European Commission. Taking into account both the limitations of transport and the assembly sequence of JT60-SA, the cryostat is divided in two main parts, namely the cryostat base and the cryostat vessel body.

The paper is focused on the structural analyses carried out by CIEMAT to evaluate the mechanical behavior of the JT-60SA cryostat base final design, since the cryostat vessel body will be designed and manufactured in a subsequent stage.

The overall structural integrity of the cryostat base has been verified and confirmed utilizing the 'limit analysis' procedure defined in ASME code 2007 Section VIII, Div. 2. The study has been complemented by further finite element analyses that include the detail of the bolted fastenings, aimed to evaluate the mechanical behavior of the bolted joints themselves, as well as the stresses and deformations in the overall cryostat base structure.

1. Introduction

JT-60SA is a superconducting tokamak to be assembled and operated at the JAEA laboratories in Naka (Japan). The tokamak is designed, manufactured and operated under the funding of the Broader Approach Agreement (between the government of Japan and the European Commission) and of the Japan Fusion National Programme; JT-60SA aims to prepare, support and complement the ITER experimental programme. The European contribution to the JT-60SA is, for a large fraction, procured by France, Germany, Italy, Spain and Belgium. Within this framework, Ciemat is in charge of the design and manufacturing of the JT-60SA cryostat.

The JT-60SA cryostat is the stainless steel vacuum vessel (14 m diameter and 16 m height) which encloses the tokamak and provides a vacuum environment, necessary to limit the transmission of thermal loads to the components at cryogenic temperature [1,2]. It has to support both the external pressure load in normal operation and an accidental overpressure.

For transport and assembly reasons the JT-60SA cryostat consists of two main parts, namely the cryostat base (CB) and the cryostat vessel body (CVB). The CB is also divided into sectors, as shown in Fig. 1, that will have to be assembled on-site by means of bolted fasteners.

The CB, which acts as the foundation of the tokamak, has the most demanding structural requirements since it supports the mechanical loads applied by the vacuum vessel (VV), the superconducting magnets and the CVB itself.

The paper summarizes the finite element structural analyses performed by Ciemat, using ANSYS code, to evaluate and validate the mechanical behavior of the CB final design.

The overall structural integrity of the cryostat base is verified and confirmed by the 'limit analysis' approach, according to ASME 2007 VIII rules and procedures. The method is based on the application of all design loads, with specified combinations and safety factors, and the performance of nonlinear analyses with elastic-perfectly plastic material properties, allowing a more realistic structural assessment in presence of localized stress concentrations. This study is complemented by finite element analyses, modeling the material in elastic regime and detailing the fasteners nonlinear behavior, in order to evaluate the performance of bolted connections, as well as the stress distribution and deformation of the overall structure.

* Corresponding author. Tel.: +34 91 346 6637; fax: +34 91 346 6124.
E-mail address: esther.rincon@ciemat.es (E. Rincón).

0920-3796/$ – see front matter © 2011 Elsevier B.V. All rights reserved.
doi:10.1016/j.fusengdes.2011.01.008

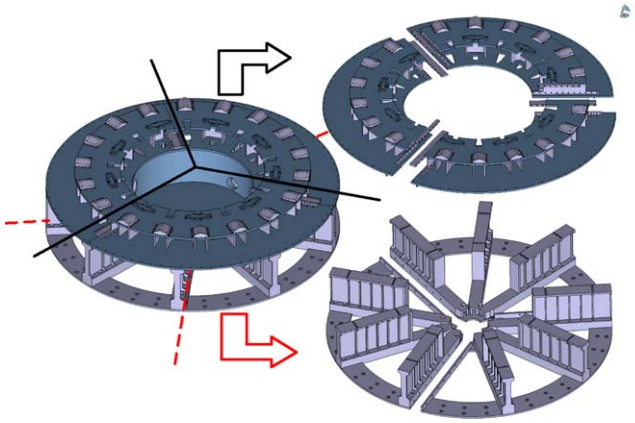

Fig. 1. Cryostat base division into sectors.

2. Design loads

The CB is designed to withstand the following loading conditions, as identified in the JT-60SA Plant Integration Document (PID) [3]:

Pressure (*P*). Vacuum condition (−0.1 MPa) inside the cryostat for normal operation, and 0.12 MPa absolute internal pressure in case of accidental loss of coolant.

Weight (*W*). Weight of the CVB (350 ton), the VV (400 ton), the magnets and thermal shields (800 ton).

Temperature (*T*). Thermal loads due to the magnets cool down at 4 K and the VV temperature, in both baking (473 K) and normal operation (323 K).

Vertical Displacement Event (*VDE*) [4]. These values are taken from the JT-60SA PID [3], where the vertical load on VV is ±7.5 MN and the horizontal one is ±2.5 MN. The loads on the toroidal field coils (TFC) will be equal and opposite to those on the VV. However, for an equivalent static analysis, forces with dynamic amplification factors should be applied, leading to the vertical load of ±7.5 MN on the VV and ±5.25 MN on the TFC, and the horizontal load of ±1.25 MN on the VV and ±1.25 MN on the TFC.

Full Seismic Event (*S*). The assumptions to calculate these loads are based on previous modal analyses performed for the whole JT-60SA, and for the TFC [5], and VV [6]. Main horizontal natural frequencies in TFC and VV are 3.4 Hz and 6.25 Hz, respectively, while verticals are 6.6 Hz in TFC and 20.86 Hz in the VV. According to the Acceleration Design Response Spectra included in the PID, these values lead to the applied accelerations in both the horizontal direction (5.83 m/s^2 in the TFC, and 8 m/s^2 in the VV) and vertical direction (2.72 m/s^2 in the TFC, and 1.33 m/s^2 in the VV).

Complementary analyses have been performed, including the TFC and the VV, in order to get the thermal and mechanical loads transmitted by these components to the CB.

3. Limit analysis

The limit analysis determines a lower bound to the limit load of a component, so providing an alternative to elastic analysis and stress linearization and the satisfaction of primary stress limits.

The theory of limit analysis defines the limit of a structure as the solution of a numerical model with the following requirements: the material model has to be elastic–perfectly plastic with a specified yield strength; the strain–displacement relations are those of small displacement theory; and equilibrium is to be satisfied in the undeformed configuration.

If convergence is achieved for every load case combination, then the component is stable under the applied loads.

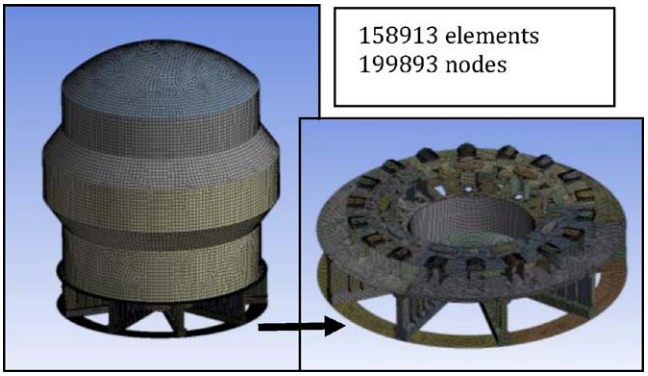

Fig. 2. General view of the CB model for limit analysis.

Table 1
Loading cases for limit analysis.

Loading case	Load combination
1	1.5 (P + W)
2	1.3 (P + W + T) + 1.7VDE
3	1.3 (P + W) + 1.1VDE
4	1.3 (P + W) + 1.1S + 1.1VDE

3.1. Numerical model

The finite element model developed for limit analysis is shown in Fig. 2. Bolted flanges and the corresponding bolts are not included in this model, according to the requirements defined in the ASME Code. The model consists of 158,913 elements and 199,893 nodes, being most of them the shell element SHELL181 (4-Node Quadrilateral Shell). Solid elements SOLID187 (10-Node Tetrahedron) and SOLID186 (20-Node Hexahedron) have been used only for the base of the magnet legs and the VV supports.

Material properties introduced in the model for limit analysis correspond to those of the SS304 elastic–perfectly plastic behavior.

3.2. Load case combinations

Loading case combinations, with the corresponding amplification factors, are taken from the Table 5.4 in ASME code 2007 Section VIII, according to the design loads defined in Section 2. They result in the loading cases summarized in Table 1.

3.3. Results

Only loading cases 2 and 4 included in Table 1 show localized areas in which the material plasticizes due to thermal and seismic loads, respectively. In the remaining cases 1 and 3 just elastic strains are shown, as the peak stresses are lower than the minimum yield stress of the material. Anyway, convergence is achieved for every loading case. Therefore, according to ASME code, the structural integrity of the cryostat base is assured. Nonetheless, the areas of concern, located in the ribs of the double ring, have been reinforced, as can be observed in the detail of Fig. 6.

4. Cryostat base structural analysis including bolted joints

The CB is divided in seven sub-parts, due to transport limitations, which are assembled by bolted fasteners, as shown in Fig. 3.

The main objective of the present analysis is to evaluate the behavior of the CB bolted joints. The critical connections are the bolted joints in the double ring shown in Fig. 3, as they have to assure both the vacuum sealing in the lower plate of the double ring and the tolerances in the upper one.

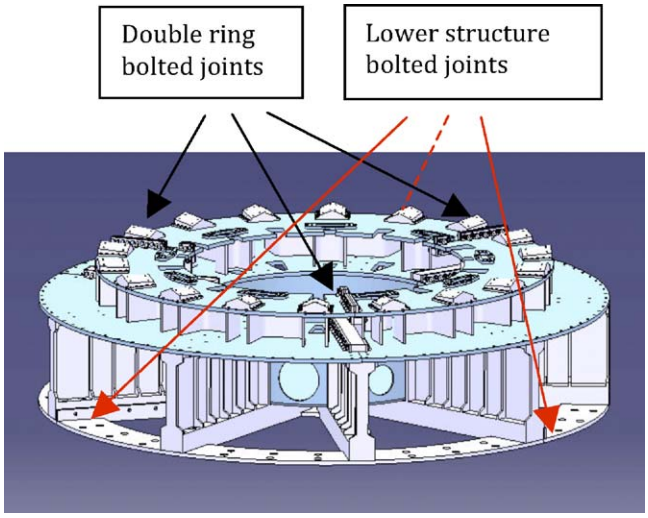

Fig. 3. Bolted fasteners in the cryostat base.

Table 2
Applied preload in bolts.

	M33	M48	M52	M64
Yield strength (MPa) min.	515	515	450	450
Root area (mm^2)	647.2	1376.6	1652.2	2519.5
Preload (N)	249,947	464,608	557,629	850,344

4.1. Bolts preload

Spacers and flanges in fasteners are made of SS 304, like the rest of the cryostat base structure, while the bolts correspond to the standard A4-80 (UNS S31600).

The applied preload in bolts corresponds to 75% of minimum yield strength, according to ITER Magnet Structural Design Criteria [7], as shown in Table 2. Values for yield strength are taken from ASME code.

4.2. Contact model

A second finite element model including every bolted joint is needed to evaluate the behavior of the bolted connections, as shown in Fig. 4. It has been developed with solid elements, and considering elastic material properties. The number of total elements rises to 1,202,754, with 2,975,231 nodes, including contact elements.

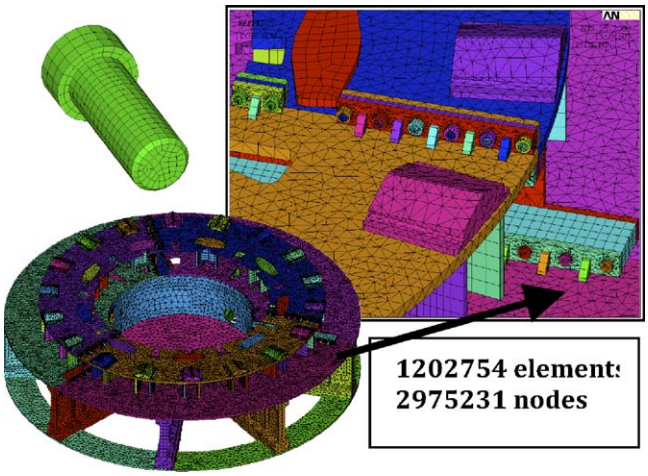

Fig. 4. Detailed view of CB model with bolted fasteners.

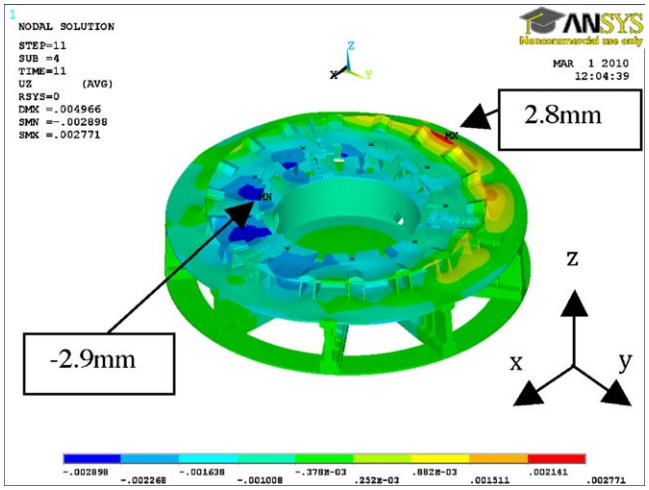

Fig. 5. Maximum vertical displacements.

From the above number of total elements, 975,645 correspond to solid elements, being the rest mainly contact ones. Moreover, 478,677 of the solid elements are only due to the bolts, what gives an idea of the influence of the bolted joints in the complexity of the model. The solid elements used are SOLID187 (10-Node Tetrahedron) and SOLID186 (20-Node Hexahedron), both with intermediate node in the edges.

4.3. Loading cases

According to the design loads described in Section 2, the analysis has considered the dead weight and vacuum pressure, in addition to the four possible combinations due to VDE or Seismic loads. Thermal load has also been added to every VDE combination, but seismic load cases have been calculated both with and without thermal loads. Therefore, twelve different loading cases have been analyzed.

4.4. Results: stress/strain distribution

Both maximum stress and strain are in the seismic loading case with thermal load, when the seismic load is applied in the positive *x* and *z* global axes.

The outcome for vertical displacements is shown in Fig. 5. Maximum displacements are 2.8 mm upward and −2.9 mm downward, that are acceptable, considering the design requirements of the cryostat base.

The outcome for Von Mises stress distribution is shown in Fig. 6, with a peak stress of 393 MPa, lower than the acceptable limit according to ASME code 3Sm = 414 MPa, what supports the stability of the CB structure, already assured by the Limit Load analysis included in Section 3.

Stresses in bolted joints are not included in Fig. 6. When the stress distribution in the bolted fasteners is analyzed, the resulting stresses are due just to the applied preload in bolts, being the variation of these stresses negligible when all the design loads are applied.

4.5. Results: bolted joint contact

Bolted joint contact analysis is focused on the double ring connections, as they have to assure the vacuum integrity in the lower plate of the double ring and the right assembly of the upper one.

When considering VDE and seismic loading cases with thermal loads, the lower plate is near full contact, while the upper one shows a gap that grows towards the outer diameter of the ring, mainly due

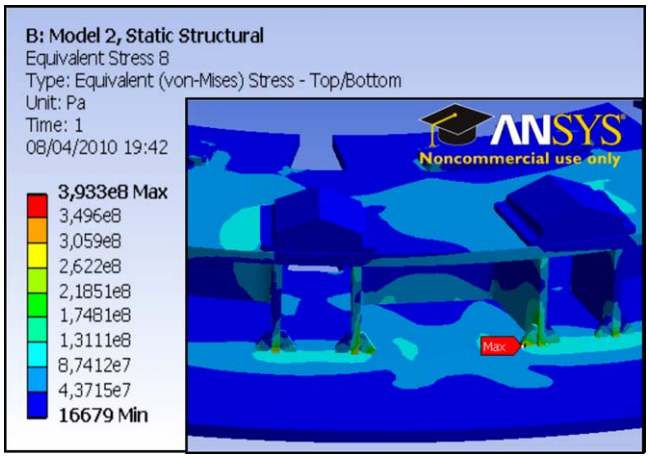

Fig. 6. Maximum stress in CB structure, in Pa.

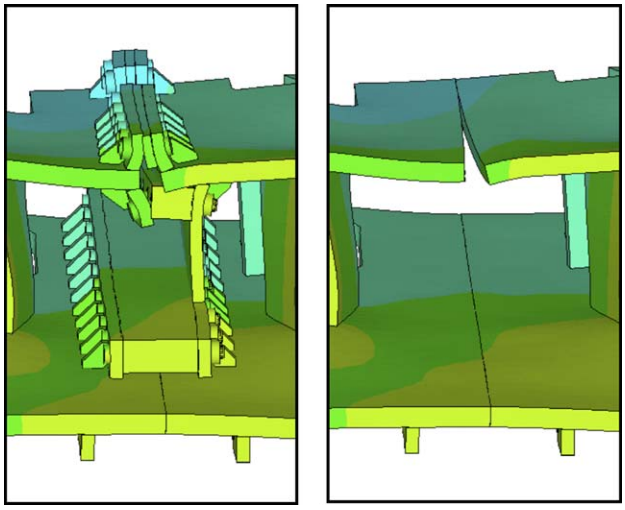

Fig. 7. Bolted joint behavior. Amplification factor = 100.

to thermal deformations. Fig. 7 includes two different views of the same union, with and without the union flanges respectively, with an amplification factor of 100.

The upper plate contact increases the gap linearly from zero in the inner part to 0.9 mm in the outer part, both in seismic and VDE loads, due mainly to thermal strains. This behavior is acceptable from a mechanical point of view, as they are already inside the cryostat vacuum. When thermal loads are not applied, the contact area increases, reducing the maximum gap to 0.09 mm, so highlighting the influence of the thermal loads.

The maximum gap in the lower plate takes place in the seismic loading cases, showing a maximum value of only 0.018 mm when thermal loads are applied. But when thermal loads are removed, the contact pressure in the lower plate decreases slightly, so that the gap increases up to 0.038 mm (Fig. 8). Nonetheless, it has to be taken into account that this gap is located just in a small area, in

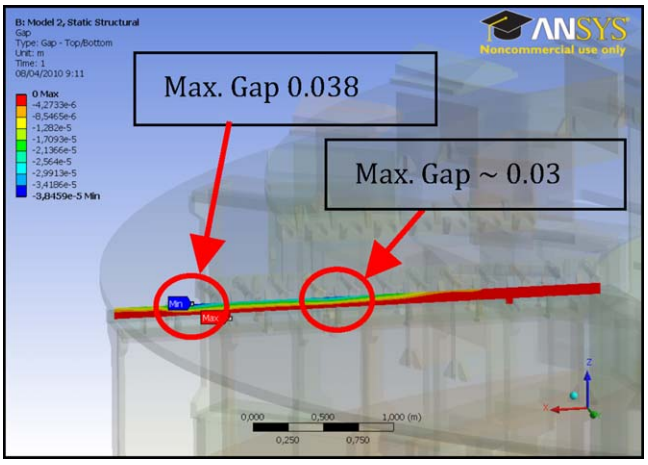

Fig. 8. Maximum contact gap in the lower plate.

the upper part of the contact, while the lower part is completely compressed. In addition, the gap values are of the same order of magnitude than the numerical tolerances of the contact, so they cannot be considered literally. Therefore, it can be confirmed that the current design assures the vacuum sealing of the CB structure.

5. Conclusions

The structural integrity of the cryostat base is assured, according to the ASME code, as convergence is achieved for every loading case proposed in the limit analysis. This is also validated by a complementary structural analysis, showing a peak value of 393 MPa, lower than the acceptable ASME stress limit.

On the other hand, the stress variation in the bolts after applying all the loads is negligible. This means that the bolts and the shear keys are working properly; so that the resulting stresses are mainly due to the initial preload for which they are designed.

The strains and deformations have been evaluated too, showing vertical displacements of the whole structure lower than 3 mm, which is acceptable according to the design criteria.

And finally the contact analysis shows that the behavior of the double ring fasteners is also acceptable, assuring both the vacuum sealing in the lower plate, and small deformations in the upper one.

References

[1] Y.K. Shibama, S. Sakurai, K. Masaki, A.M. Sukekawa, A. Kaminaga, A. Sakasai, et al., Conceptual design of JT-60SA cryostat, Fusion Engineering and Design 83 (December (10–12)) (2008) 1605–1609.
[2] J. Botija, J. Alonso, J. Barrera, G. Fernández, P. Medrano, M. Pérez, et al., JT60-SA cryostat design and assembly, in: 26th SOFT, Porto, Portugal, October, 2010.
[3] JT-60SA Plant Integration Document (PID) Version 2.4, JT-60SA DMS Number BA_D_222UJY. 21-05-10.
[4] M. Verrecchia, Simulation of VDE's in JT60SA, 2008, JT-60SA DMS Number 22CBZW.
[5] L. Meunier, Mechanical assessment of the JT-60SA TF Coils during seismic event, in: 26th SOFT, Porto, Portugal, October, 2010.
[6] Y.K. Shibama, Update of design and analysis of VV and its supports, 2009, JT-60SA DMS Number 223ENF.
[7] N. Mitchell, C. Jong, A. Alekseev, Magnet Structural Design Criteria. Part III. Bolts, Keys Supports and Special Components, 2009, ITER IDM Number ITER_D_2FKTTG V.1.2.